

Accepted Manuscript

Design and synthesis of novel xanthine derivatives as potent and selective A₂B adenosine receptor antagonists for the treatment of chronic inflammatory airway diseases

Sujay Basu, Dinesh A. Barawkar, Vidya Ramdas, Meena Patel, Yogesh Waman, Anil Panmand, Santosh Kumar, Sachin Thorat, Minakshi Naykodi, Arnab Goswami, B. Srinivasa Reddy, Vandna Prasad, Sandhya Chaturvedi, Azfar Quraishi, Suraj Menon, Shalini Paliwal, Abhay Kulkarni, Vikas Karande, Indraneel Ghosh, Syed Mustafa, Siddhartha De, Vaibhav Jain, Ena Ray Banerjee, Sreekanth R. Rouduri, Venkata P. Palle, Anita Chugh, Kasim A. Mookhtiar

PII: S0223-5234(17)30268-4

DOI: [10.1016/j.ejmech.2017.04.014](https://doi.org/10.1016/j.ejmech.2017.04.014)

Reference: EJMECH 9361

To appear in: *European Journal of Medicinal Chemistry*

Received Date: 15 November 2016

Revised Date: 1 April 2017

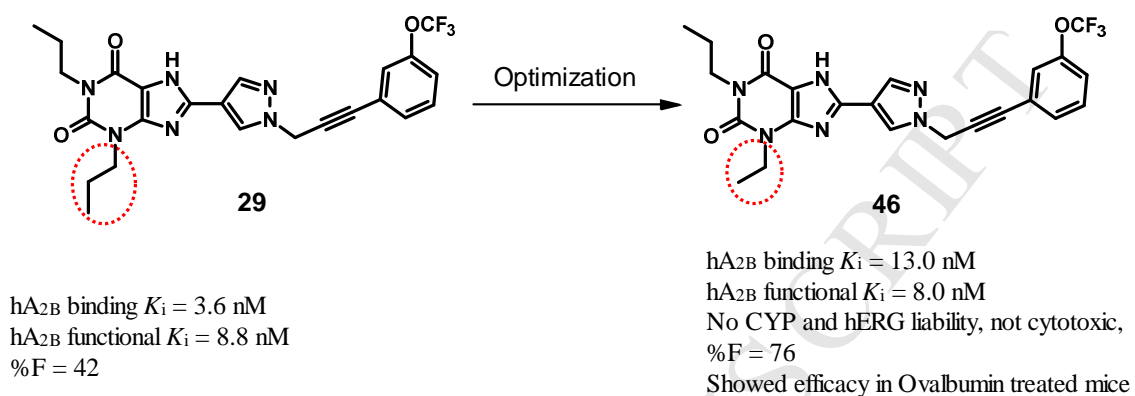
Accepted Date: 7 April 2017

Please cite this article as: S. Basu, D.A. Barawkar, V. Ramdas, M. Patel, Y. Waman, A. Panmand, S. Kumar, S. Thorat, M. Naykodi, A. Goswami, B.S. Reddy, V. Prasad, S. Chaturvedi, A. Quraishi, S. Menon, S. Paliwal, A. Kulkarni, V. Karande, I. Ghosh, S. Mustafa, S. De, V. Jain, E.R. Banerjee, S.R. Rouduri, V.P. Palle, A. Chugh, K.A. Mookhtiar, Design and synthesis of novel xanthine derivatives as potent and selective A₂B adenosine receptor antagonists for the treatment of chronic inflammatory airway diseases, *European Journal of Medicinal Chemistry* (2017), doi: 10.1016/j.ejmech.2017.04.014.

This is a PDF file of an unedited manuscript that has been accepted for publication. As a service to our customers we are providing this early version of the manuscript. The manuscript will undergo copyediting, typesetting, and review of the resulting proof before it is published in its final form. Please note that during the production process errors may be discovered which could affect the content, and all legal disclaimers that apply to the journal pertain.



Graphical abstract



Design and Synthesis of Novel Xanthine Derivatives as Potent and Selective A_{2B} Adenosine Receptor Antagonists for the treatment of Chronic Inflammatory Airway Diseases

Sujay Basu*, Dinesh A. Barawkar, Vidya Ramdas, Meena Patel, Yogesh Waman, Anil Panmand, Santosh Kumar, Sachin Thorat, Minakshi Naykodi, Arnab Goswami, B. Srinivasa Reddy, Vandna Prasad, Sandhya Chaturvedi, Azfar Quraishi, Suraj Menon, Shalini Paliwal, Abhay Kulkarni, Vikas Karande, Indraneel Ghosh, Syed Mustafa, Siddhartha De, Vaibhav Jain, Ena Ray Banerjee, Sreekanth R. Rouduri, Venkata P. Palle, Anita Chugh, Kasim A. Mookhtiar*

Advinus Therapeutics Ltd., Drug Discovery Facility, Quantum Towers, Plot-9, Phase-I, Rajiv

Gandhi Infotech Park, Hinjawadi, Pune 411 057, India

Abstract. Adenosine induces bronchial hyperresponsiveness and inflammation in asthmatics through activation of A_{2B} adenosine receptor (A_{2B}AdoR). Selective antagonists have been shown to attenuate airway reactivity and improve inflammatory conditions in pre-clinical studies. Hence, the identification of novel, potent and selective A_{2B}AdoR antagonist may be beneficial for the potential treatment of asthma and Chronic Obstructive Pulmonary Disease (COPD). Towards this effort, we explored several prop-2-ynylated C8-aryl or heteroaryl substitutions on xanthine chemotype and found that 1-prop-2-ynyl-1*H*-pyrazol-4-yl moiety was better tolerated at the C8 position. Compound **59**, exhibited binding affinity (K_i) of 62 nM but was non-selective for A_{2B}AdoR over other AdoRs. Incorporation of

* Corresponding author. Tel.: +91 20 66539600; fax: +91 20 66539620.

E-mail address: sujay.basu@advinus.com

* Corresponding author. Tel.: +91 20 66539600; fax: +91 20 66539620.

E-mail address: kasim.mookhtiar@advinus.com

substituted phenyl on the terminal acetylene increased the binding affinity (K_i) significantly to <10 nM. Various substitutions on terminal phenyl group and different alkyl substitutions on N-1 and N-3 were explored to improve the potency, selectivity for A_{2B} AdoR and the solubility. In general, compounds with *meta*-substituted phenyl provided better selectivity for A_{2B} AdoR compared to that of *para*-substituted analogs. Substitutions such as basic amines like pyrrolidine, piperidine, piperazine or cycloalkyls with polar group were tried on terminal acetylene, keeping in mind the poor solubility of xanthine analogs in general. However, these substitutions led to a decrease in affinity compared to compound **59**. Subsequent SAR optimization resulted in identification of compound **46** with high human A_{2B} AdoR affinity ($K_i = 13$ nM), selectivity against other AdoR subtypes and with good pharmacokinetic properties. It was found to be a potent functional A_{2B} AdoR antagonist with a K_i of 8 nM in cAMP assay in h A_{2B} -HEK293 cells and an IC_{50} of 107 nM in IL6 assay in NIH-3T3 cells. Docking study was performed to rationalize the observed affinity data. Structure-activity relationship (SAR) studies also led to identification of compound **36** as a potent A_{2B} AdoR antagonist with K_i of 1.8 nM in cAMP assay and good aqueous solubility of 529 μ M at neutral pH. Compound **46** was further tested for *in vivo* efficacy and found to be efficacious in ovalbumin-induced allergic asthma model in mice.

Keywords: Adenosine; cAMP; Bioavailability; Propargyl; Heteroaryl; Human liver microsomes

1. Introduction

Adenosine plays numerous important physiological roles via a family of four G-protein coupled receptors (GPCR), namely A_1 , A_{2A} , A_{2B} and A_3 adenosine receptors (AdoRs) [1]. A_1 and A_{2A} AdoRs are stimulated by low nanomolar adenosine concentrations, while micromolar concentrations of adenosine are required for the activation of A_{2B} and A_3 AdoRs [2]. The low affinity AdoRs (A_{2B} and A_3) are activated only under stressful conditions wherein adenosine levels are elevated to micromolar concentrations. Increased levels of adenosine have been reported under pathophysiological conditions,

such as hypoxic or ischemic conditions, after massive cell death, or as a consequence of inflammatory processes [3,4]. Rodent and human A_{2B} AdoRs share 86-87% amino acid sequence homology [5]. The A_{2B} AdoRs show a ubiquitous distribution, with highest levels observed in the cecum, colon, bladder, mast cells, hematopoietic cells, and lung, while lower levels are detected in other organs, such as brain and liver [6].

Apart from the differences in affinity to adenosine, the receptors also differ in their signaling mechanism. A_1 and A_3 AdoRs mediate inhibition of adenylate cyclase through G_i coupled pathway, whereas A_{2B} and A_{2A} stimulate adenylate cyclase activity via G_s coupling and result in increased intracellular cAMP levels [5]. In addition, coupling of A_{2A} and A_{2B} AdoRs to phospholipase C via G_q , resulting in mobilization of intracellular calcium and direct coupling to calcium channels (stimulation of calcium influx), have also been reported [7-9].

Adenosine has been shown to cause mast cell degranulation [10], vasodilation [11], chloride secretion in epithelial cells [12, 13], growth inhibition of smooth muscle cells [14], and stimulation of glucose production in rat hepatocytes [15] and stimulate VEGF secretion [16] via activation of A_{2B} AdoR. A_{2B} AdoR antagonists, therefore, can potentially be used as therapeutic agents for the treatment of asthma and chronic obstructive pulmonary disease [4, 17-19] type II diabetes [15], cystic fibrosis [12], inflammatory bowel disease [13] and cancer [20].

Adenosine induces bronchoconstriction in asthmatic patients but not in normal people [21, 22]. In addition, adenosine levels are elevated in the bronchoalveolar lavage fluid and exhaled breath condensates of asthmatic patients [23, 24] and adenosine deaminase deficient mice show evidence of bronchioli remodelling and emphysema-like lesions [25,26]. The mechanism of this adenosine-mediated damage lies with the activation of A_{2B} AdoR on human mast cells, which in turn leads to mast cell degranulation and release of inflammatory cytokines IL-4, IL-8 and IL-13 [27]. A_{2B} AdoR activation also increases the expression and release of IL-6 and TNF- α in bronchial epithelial cells [28] and this indicates that A_{2B} AdoR play a key role in the pathogenesis of inflammatory lung disease. There is also evidence that A_{2B} AdoR is the predominant AdoR expressed in bronchial smooth muscle cells, and its

activation increases the expression and release of IL-6 and monocytic chemotactic peptide-1(MCP-1) [29] and is implicated in airway remodeling. In human lung fibroblasts, activation of A_{2B}AdoR induces the release of IL-6 and differentiation of fibroblasts to myofibroblasts [30].

On account of all the evidence that implicates A_{2B}AdoR activation in inflammatory lung diseases such as asthma, COPD and fibrosis, a lot of research has been carried out with the goal of identifying potent and selective A_{2B}AdoR antagonists to provide a novel approach to the management and treatment of asthma and COPD.

The alkylxanthines theophylline **1** and enprofylline **2** (Figure 1), are weak, non-selective AdoR antagonists used therapeutically for the treatment of asthma [31, 32]. The bronchodilating effect of **1** and **2** has been attributed to a selective antagonism of A_{2B}AdoR, which prompted several groups to design and test a large number of xanthine derivatives in the search for new, more potent and selective A_{2B}AdoR antagonists. During the past decade, several structure-activity relationship studies of A_{2B}AdoR antagonists have been published [33-37]. Though several potent and selective A_{2B}AdoR antagonists like MRS-1754 (**3**), MRE2029-F20 (**4**) have been reported, these compounds were highly lipophilic, possessing very low solubility and poor oral bioavailability [38, 39].

A potent and selective A_{2B}AdoR antagonist CVT-6883 (**5**) [36, 40] entered into clinics and later discontinued from Phase I clinical trials. It has shown inhibition of airway inflammation and airway reactivity induced by allergen or AMP in mouse model of allergic asthma [41]. In addition, compound **5** attenuated pulmonary inflammation, fibrosis, and alveolar airspace enlargement and reduced elevations of pro-inflammatory cytokines and chemokines, as well as mediators of fibrosis [42].

In our earlier communication we had reported a new series of xanthine derivatives [43]. The objective of present study was to identify and develop novel, potent and selective A_{2B}AdoR antagonists combined with good aqueous solubility and improving *in vivo* half life. As we were interested in synthesizing and testing novel xanthine derivatives, first we explored different propargylated aryl and heteroaryl groups at C8 position of xanthine and identified 8-(1-prop-2-ynyl-1*H*-pyrazol-4-yl)-xanthine as a potential core for SAR studies. Herein, we discuss the structure-activity relationship (SAR) studies carried out on 8-(1-

prop-2-ynyl-1*H*-pyrazol-4-yl)-xanthine towards identification of novel, potent and selective A_{2B} AdoR antagonists with good oral bioavailability.

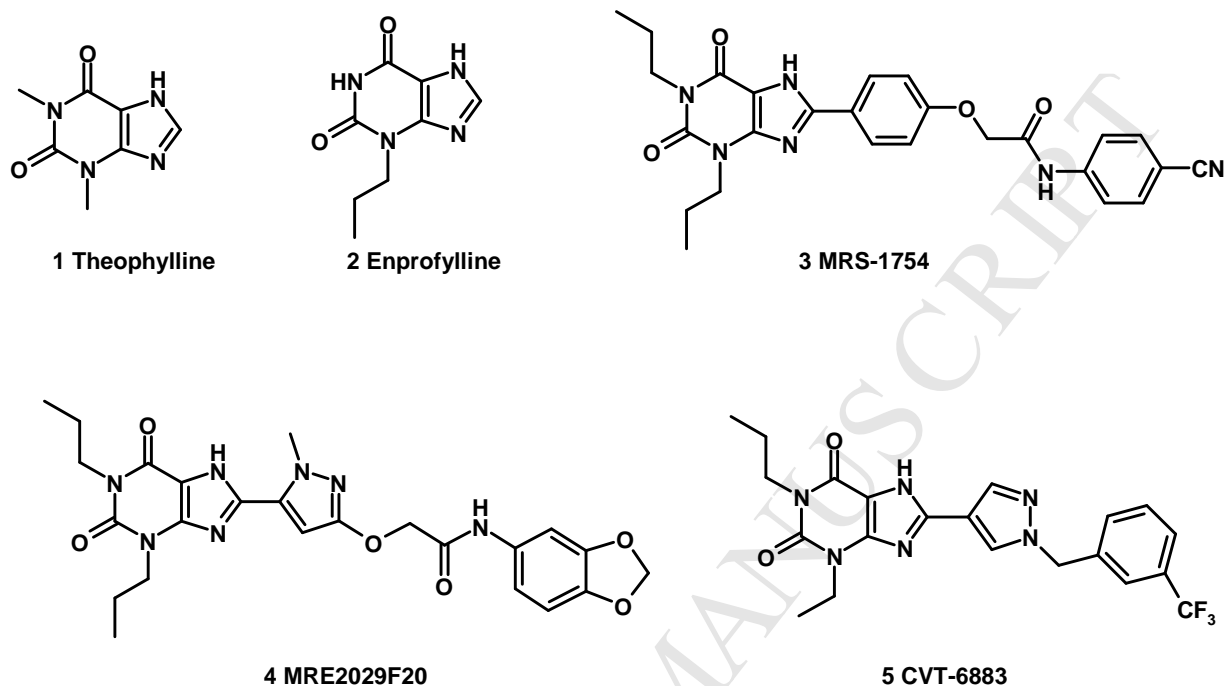


Figure 1. Representative Structures of Xanthine Based A_{2B} AdoR Antagonists

2. Results and discussion

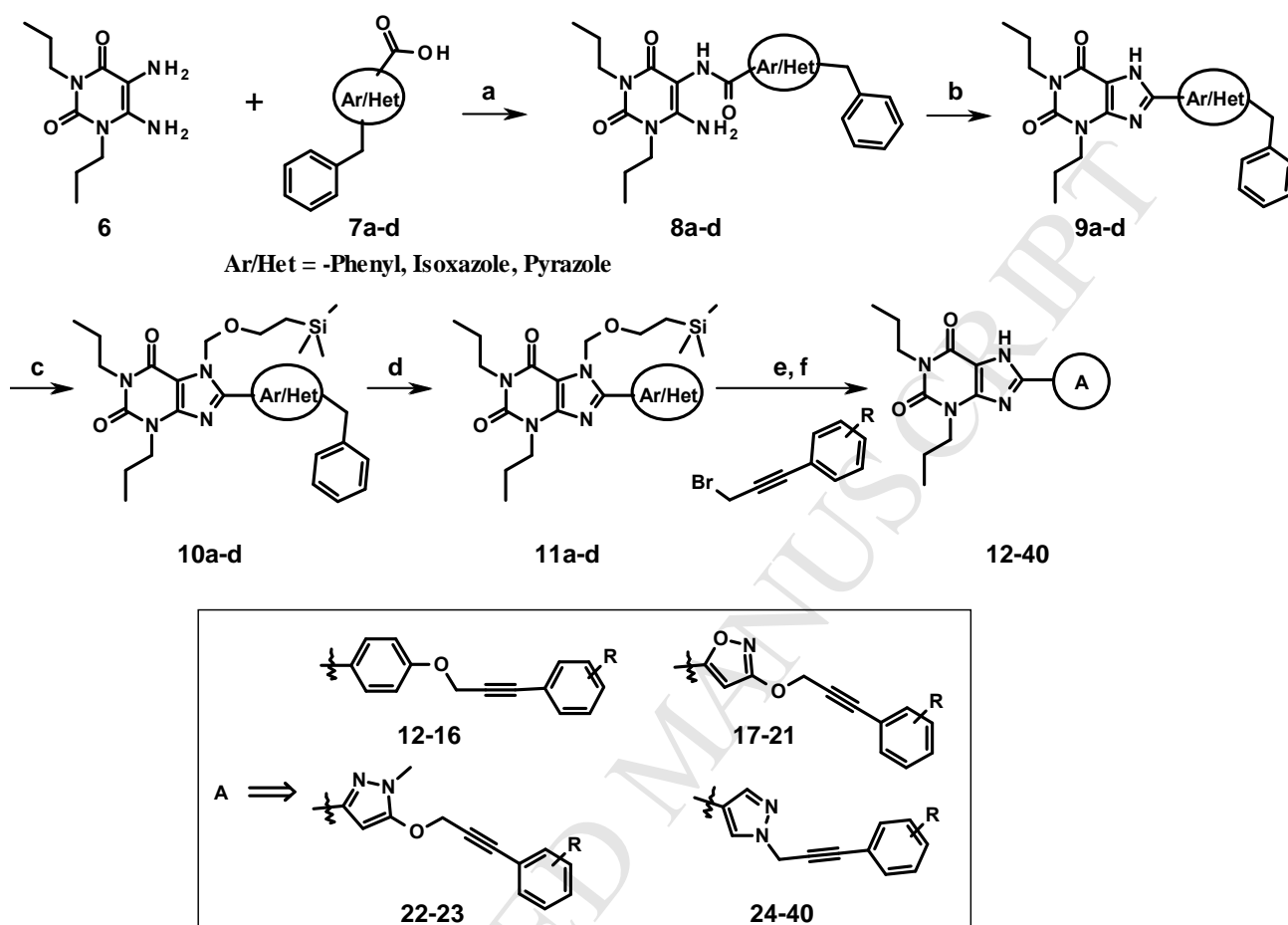
2.1. Chemistry

The key intermediates 8-phenyl-, 8-isoxazolyl-, 8-(1*H*-pyrazol-3-yl)- and 8-(1*H*-pyrazol-4-yl)-1,3-dipropyl xanthines were prepared by classical method starting from 1,3-dipropyl-5,6-diaminouracil **6** (Scheme 1) [36]. The diamino uracil **6** was coupled with phenyl carboxylic acid **7a**, isoxazole carboxylic acid **7b**, pyrazole-3- or pyrazole-4-carboxylic acids **7c** or **7d**, using *N*-(3-dimethylaminopropyl)-*N*-ethylcarbodiimide hydrochloride (EDCI) in methanol at room temperature to obtain corresponding carboxamide derivatives **8a-d**. Subsequent ring closure of these derivatives was performed by refluxing **8a-d** with 10% sodium hydroxide in methanol to afford 8-substituted xanthine derivatives **9a-d**. The *N*-7 position of **9a-d** was protected with 2-(trimethylsilyl)ethoxymethylchloride (SEM-Cl) using potassium

carbonate in dimethylformamide to furnish **10a-d** which on debenzoylation using hydrogen and 10% Pd/C provided the key intermediates **11a-c** with “O” and **11d** with “N” as a handle for further derivatization [36]. These compounds were alkylated with various substituted (3-bromo-prop-1-ynyl)-benzene derivatives using potassium carbonate in acetone at reflux temperature to provide the silyl protected xanthine derivatives which on silyl deprotection with 2N HCl furnished the final compounds **12-40** in good yields (28-99%) Scheme 1.

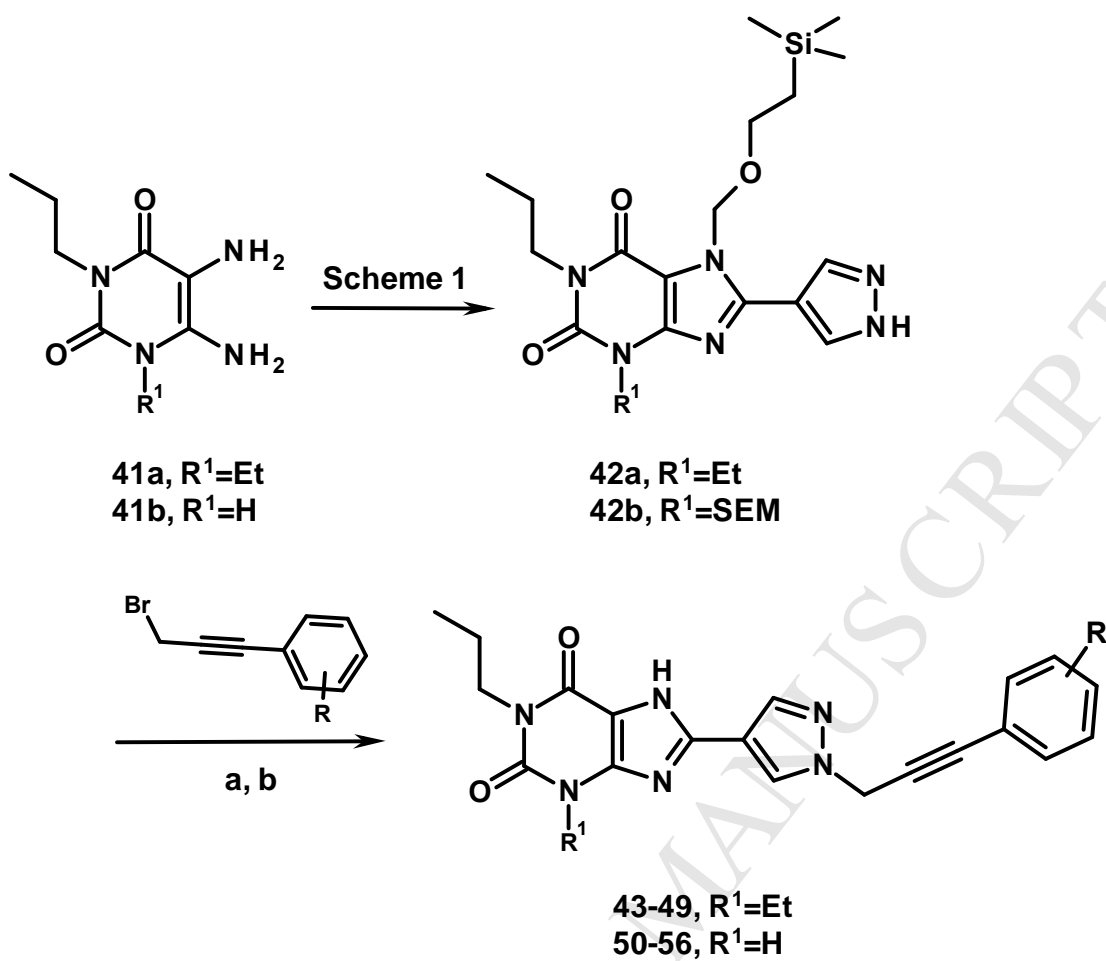
In a similar fashion, various N-1, N-3 differentially substituted xanthine derivatives were prepared by starting from 1-ethyl-3-propyl-5,6-diaminouracil **41a** or 1H-3-propyl-5,6-diaminouracil **41b** [44]. The key intermediates, 3-ethyl-1-propyl-8-(1*H*-pyrazol-4-yl)-xanthine **42a** or 1-propyl-8-(1*H*-pyrazol-4-yl)-xanthine **42b** were prepared (Scheme 2) by following the synthetic sequence as described in Scheme 1. The alkylation of **42a** or **b** with various phenyl substituted propargyl bromides using standard alkylation conditions followed by N-7 silyl deprotection with 2N HCl furnished **43-56** in good yields (11-85%).

Propargyl and 2-butyne substituted 8-(1*H*-pyrazol-4-yl)-xanthine derivatives **59** and **60** were prepared (Scheme 3) by alkylation of intermediate **11d** with corresponding bromo compounds using potassium carbonate in acetone at reflux condition, followed by N-7 deprotection of the resulting silyl protected compounds **57** and **58** with 2N HCl in ethanol at reflux condition. Compounds substituted with basic amino moiety on terminal acetylene **61-66** were prepared (Scheme 4) by treating the 1,3-dipropyl-8-(1-prop-2-ynyl-1*H*-pyrazol-4-yl)-xanthine **57** with formaldehyde solution and acyclic or heterocyclic amines in presence of CuI in dimethylsulfoxide at room temperature followed by N-7 silyl deprotection. The compounds, 8-{1-[3-(1-Hydroxy-cycloalkyl)-prop-2-ynyl]-1*H*-pyrazol-4-yl}-xanthine derivatives, **67** and **68** were also obtained in a similar fashion. The reaction of intermediate **57** with cyclopentanone or cyclohexanone in the presence of lithiumhexamethyl disilazide in tetrahydrofuran at low temperatures followed by N-7 silyl deprotection furnished the compounds **67** and **68**, Scheme 4.

Scheme 1. Synthesis of compounds **12-40**^a

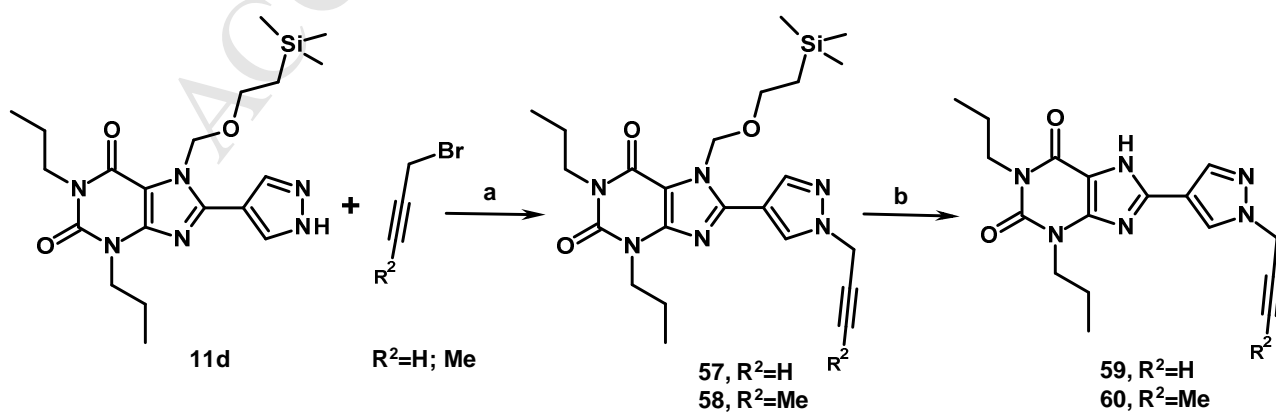
^aReagents and conditions: (a) EDCI, MeOH, r.t.; (b) 10% NaOH, MeOH, reflux; (c) SEM-Cl, K₂CO₃, DMF, r.t.; (d) H₂, 10% Pd/C, MeOH:DCM (2:1), r.t.; (e) K₂CO₃, acetone, 50 °C; (f) 2N HCl, ethanol, 80 °C

Scheme 2. Synthesis of compounds **43-49** and **50-56**^a



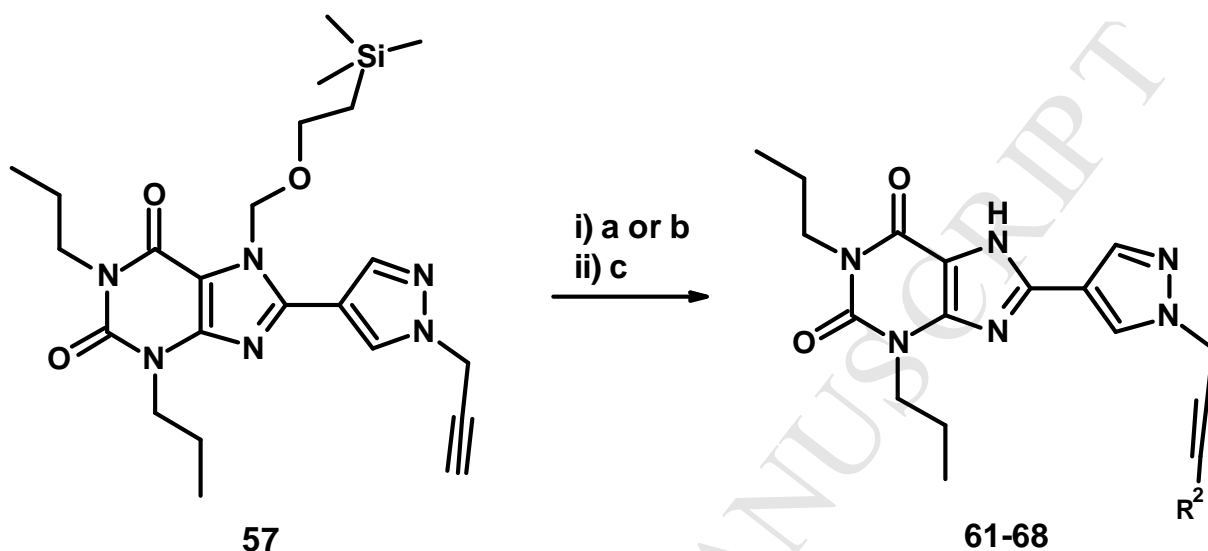
^aReagents and conditions: (a) K₂CO₃, acetone, 50 °C; (b) 2N HCl, ethanol, 80 °C

Scheme 3. Synthesis of compounds **59-60**^a



^aReagents and conditions: (a) K_2CO_3 , acetone, 50 °C; (b) 2N HCl, ethanol, 80 °C

Scheme 4. Synthesis of compounds **61-68**^a



^aReagents and conditions: (a) 37% HCHO solution, amine, CuI, DMSO, r.t.; (b) LHMDS, cyclopentanone or cyclohexanone, THF, -78 to 20 °C; (c) 2N HCl, ethanol, 80 °C

2.2. Biological activity

As we were interested in synthesizing and testing novel derivatives of xanthine with propargylated aryl and heteroaryl groups at C8 position, we first explored different aryl and heteroaryl groups at the C8 position of xanthine. Herein, we discuss the structure-activity relationship (SAR) of compounds **12-25** with phenyl, isoxazolyl, 3-pyrazolyl and 1*H*-4-pyrazolyl substitution at the C8 position (Table 1). Compounds **12-16** having phenyl, pyridyl (structure not shown), and compounds **22, 23** having 3-pyrazolyl substitutions at C8 position were found to be inactive or showed low binding affinity for A_{2B}AdoR, indicating that phenyl, pyridyl and 3-pyrazolyl are not suitable at C8 of xanthine. These compounds also showed poor solubility. When isoxazolyl was placed at C8 of xanthine, compounds **17** and **18** with small substitution like *m*-F and *p*-F on terminal phenyl ring showed moderate binding affinity of 55 and 15 nM, respectively, for A_{2B}AdoR. Compounds **19-21** with larger substituents such as

trifluoroalkyl or trifluoroalkoxy substitution on terminal phenyl ring were inactive or showed low affinity for A_{2B}AdoR. 4-Pyrazolyl, between C8 of xanthine and *m*-F and *p*-F (**24** and **25**) substituted terminal phenyl ring had high binding affinity of 6.7 and 5.9 nM, respectively, for A_{2B}AdoR (Table 1). Based on the binding affinity of compounds **12-25** for A_{2B}AdoR, it was concluded that 4-pyrazolyl ring is the best structural requirement group at the C8 position. Hence, 8-(1-propargyl-4-pyrazolyl)-1,3-disubstituted xanthine derivative was selected for further SAR studies to identify a potent, selective and soluble A_{2B}AdoR antagonist.

The binding selectivity of 8-(1-propargyl-4-pyrazolyl)-xanthine analogs **24** and **25** over other AdoR subtypes A₁AdoR and A_{2A}AdoR is shown in Table 2. These compounds were not very selective for A_{2B}AdoR. Therefore, to increase the selectivity, we explored various substitutions on the terminal phenyl ring, including electron donating groups such as methyl and methoxy, electron withdrawing groups such as trifluoromethyl, trifluoromethoxy, and cyano and polar carboxylic acids and hydroxyl groups with the intention to improve solubility. The data for these compounds is tabulated in Table 2. The binding affinity of compounds **24-40** clearly indicates that substituted phenyl groups are well tolerated on the acetylene moiety, majority of compounds showing high binding affinity K_i of <10 nM for A_{2B}AdoR, irrespective of the nature of substitution (e.g. electron donating or withdrawing group), and irrespective of the position of substitution (ortho, meta or para on phenyl ring), as outlined in Table 2. Compound **26**, with ortho substitution of trifluoromethyl, was found to be relatively less potent ($K_i = 29$ nM), and in general, not much difference was observed between meta and para substitutions in terms of binding affinity for A_{2B}AdoR. However, majority of compounds with para substitution showed modest selectivity over A_{2A}AdoR with low or no selectivity over A₁AdoR (except compounds **32** and **37**). Compounds **25**, **28**, **30**, and **40** exhibited similar binding affinity for A_{2B} and A₁AdoR. Majority of compounds with meta substitutions were selective for A_{2B}AdoR over both A₁ and A_{2A}AdoRs with Majority of the compounds exhibited highl selective over A₃AdoR ($\leq 30\%$ inhibition at 1 μ M) except for compound **38**. Among these compounds, **29**, **36**, and **39** were identified as the best compounds with high affinity and selectivity for A_{2B}AdoR. It is interesting to note that polar substitution like carboxylic

acid and ester groups **36-40** were well tolerated in terms of potency for A_{2B}AdoR and selectivity over other AdoRs. Also, compound **36** with *m*-carboxylic acid substitution endowed with better aqueous solubility of 529 μ M at pH 7.4.

To further improve the selectivity over other AdoR subtypes, we have explored different substitutions at N-3 position [44]. Table 3 shows follow-up SAR where the 4-pyrazolyl at C8 and propyl at N-1 side chain was fixed and the N-3 side chain was varied with ethyl (**43-49**) or H (**50-56**). Unexpectedly, compounds **48**, **49** and **56** having carboxylic acid substitution showed lower binding affinity for A_{2B}AdoR compared to the corresponding 1,3-dipropyl derivative **36** and **40**. Consistent with dipropyl derivatives, even in the case of 1-propyl-3-ethyl-xanthine derivatives, all *para* substituted compounds **44**, **45**, **47**, **51**, **53** and **55** exhibited modest selectivity over A_{2A}AdoR and low selectivity over A₁AdoR, whereas all the *meta* substituted compounds **46**, **52**, and **54** had better selectivity over both the receptors. An exception was observed for *m*-fluoro substituted compounds **43** and **50**. Poor selectivity observed in the case of compounds **43** and **50** could be due to the presence of a smaller group like fluoro. All these compounds (**43-56**) retained high selectivity over A₃AdoR ($\leq 30\%$ inhibition at 1 μ M).

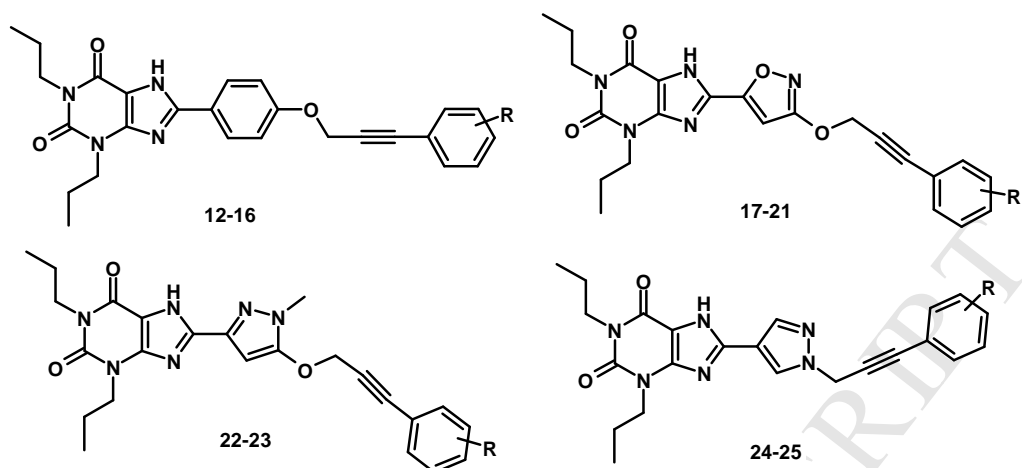
Compared to *meta* trifluoromethoxy phenyl substituted dipropyl xanthine derivative **29**, corresponding 1-propyl-3-ethyl-xanthine derivative **46** had improved selectivity as shown in Table 3. N1-monopropylated xanthine derivatives **52** and **54** had better binding affinity as well as selectivity than corresponding 1,3-dipropyl or 1-propyl-3-ethyl xanthine derivatives. However these compounds suffered from poor solubility issues.

In parallel, we pay attention towards replacement of highly lipophilic terminal aryl ring with the intension to achieve better solubility for the insoluble xanthine derivatives in combination with potency and selectivity. We replaced terminal aryl ring with small lipophilic group like H or methyl and explored polar substitutions, e.g., alcohol or basic functions on the terminal acetylene moiety as in compounds **61-68**. First, we evaluated 8-(1-prop-2-ynyl-1*H*-pyrazol-4-yl)-1,3-dipropyl xanthine **59** and 8-(1-But-2-ynyl-1*H*-pyrazol-4-yl)-1,3-dipropyl xanthine **60**, where terminal phenyl was replaced by “H” and methyl respectively for binding affinity and selectivity for A_{2B}AdoR. These compounds had modest

affinity of $K_i = 62$ and 23 nM, respectively for A_{2B} AdoR but were poorly selective (Table 4). This indicated clear need of optimization of terminal substituent for potency as well as selectivity. Compounds **61-65** with substitutions like diethylamine, pyrrolidine, piperidine, morpholine and *N*-methyl piperazine showed low affinity for A_{2B} AdoR and were non-selective over other AdoR subtypes (Table 4). However, compound **66** substituted with 4-(3-trifluoromethyl-phenyl)-piperazine showed high affinity ($K_i = 12$ nM) for A_{2B} AdoR, although it had only modest selectivity over A_1 AdoR. Compounds **67** and **68** with tertiary alcohol function also were of low affinity towards A_{2B} AdoR.

In terms of affinity and selectivity, clear SAR was demonstrated with focused optimization of 8-(1-prop-2-ynyl-1*H*-pyrazol-4-yl)-1,3-dipropyl xanthine analogs. Compounds with substituted phenyl on terminal propyne group showed high affinity compared to other non-aryl substitutions. Low or no selectivity over A_1 and A_{2A} AdoRs, as observed with most of the *para*-substituted compounds and compounds with smaller groups like fluoro (irrespective of substitution at N-3 position), could be attributed to the presence of rigid propargyl group between C8-pyrazolyl ring and terminal phenyl ring, which makes the right hand side of these compounds close to linear structures in these cases. Bringing a bulkier substitution at the meta position on the phenyl ring improved the selectivity for A_{2B} AdoR over other AdoR subtypes.

Among all compounds, compounds **29**, **36** and **46** were identified as the best in terms of binding affinity, selectivity and hence were taken forward for detailed profiling. Functional potency of these compounds was determined in hA_{2B} HEK-293 cells using cAMP assay and in NIH-3T3 cells using IL-6 assay. Compounds **29**, **36** and **46** were found to be potent A_{2B} AdoR antagonists and inhibited 5'-*N*-ethylcarboxamidoadenosine (NECA)-induced increase in cAMP with K_i of 8.8, 1.8 and 8 nM, respectively, in hA_{2B} HEK-293 cells. The compounds **29**, **36** and **46** also inhibited NECA induced IL-6 release in NIH-3T3 cells with IC_{50} of 90, 2000 and 107 nM, respectively.

Table 1. Binding Affinity of Xanthine Derivatives with C8 variation for $A_{2B}AdoR$ 

Compd	R	$hA_{2B} K_i$ (nM) ^a
12	<i>m</i> -F	> 1 μ M
13	<i>p</i> -F	NR ^b
14	<i>p</i> -CF ₃	NR ^b
15	<i>m</i> -OCF ₃	NR ^b
16	<i>p</i> -OCF ₃	>600
17	<i>m</i> -F	55
18	<i>p</i> -F	15
19	<i>m</i> -CF ₃	>600
20	<i>p</i> -CF ₃	NR
21	<i>m</i> -OCF ₃	>600
22	<i>m</i> -CF ₃	NR
23	<i>p</i> -OCF ₃	NR
24	<i>m</i> -F	6.7

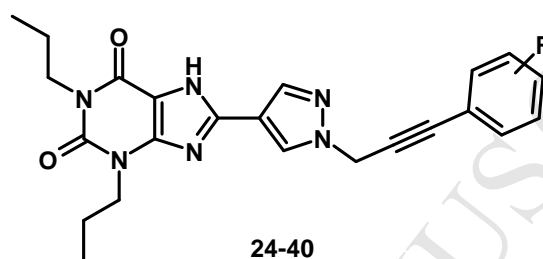
25

p-F

5.9

NR- no response. ^a Binding affinity for hA_{2B}AdoR was determined by using HEK-A_{2B} cells with [³H]-MRS-1754 as the radioligand, All data points were evaluated in triplicates. Each compound was evaluated at 8 concentrations with each data point in triplicates for *K_i* determination.

Table 2. Binding Affinity of Xanthine Derivatives with Different Substitution on Terminal Phenyl for A_{2B}, A₁, A_{2A} and A₃AdoRs

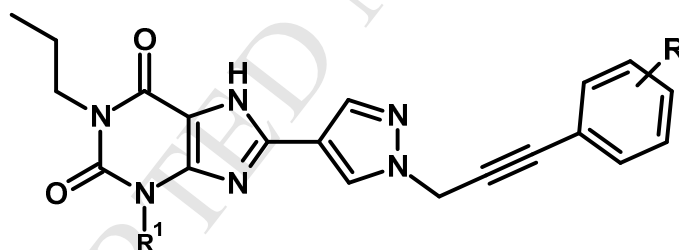


Compd	R	<i>K_i</i> (nM) hA _{2B} ^a	% Inhibition at 0.1 μM		% Inhibition at 1 μM
			hA ₁ ^a	hA _{2A} ^a	hA ₃ ^a
24	<i>m</i> -F	6.7	87	64	0
25	<i>p</i> -F	5.9	105	66	19
26	<i>o</i> -CF ₃	29	52	29	25
27	<i>m</i> -CF ₃	4.9	43	64	32
28	<i>p</i> -CF ₃	1.5	84	30	12
29	<i>m</i> -OCF ₃	3.6	39	27	6
30	<i>p</i> -OCF ₃	5.5	92	51	37
31	<i>m</i> -CN	3.7	52	84	0
32	<i>p</i> -CN	14	14	29	14
33	<i>m</i> -CH ₃	5	57	55	9
34	<i>p</i> -CH ₃	6.5	70	33	0

35	<i>m</i> -OCH ₃	6.3	57	74	21
36	<i>m</i> -CO ₂ H	5.3	20	32	0
37	<i>p</i> -CO ₂ H	17.6	19	44	25
38	<i>o</i> -CO ₂ Me	12	37	41	43
39	<i>m</i> -CO ₂ Et	7.8	29	29	0
40	<i>p</i> -CO ₂ Et	3.5	80	19	27

^aBinding affinities were determined by using membrane preparations from HEK-293 cells overexpressing the relevant human AdoR isoform. All data points were evaluated in triplicates. Each compound was evaluated at 8 concentrations with each data point in triplicates for K_i determination [45].

Table 3. Binding Affinity of N-1, N-3 Differentially Substituted Xanthine Derivatives for A_{2B}, A₁, A_{2A} and A₃AdoRs



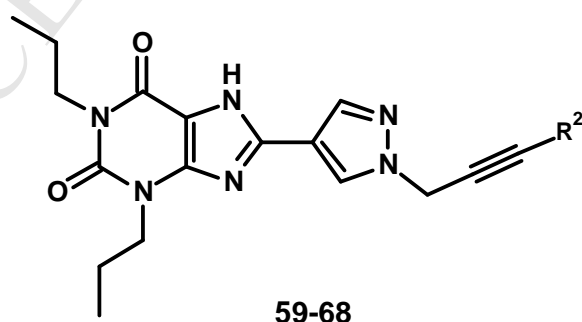
43-49, R¹=Et
50-56, R¹=H

Compd	R	K_i (nM) hA _{2B} ^a	% Inhibition at 0.1 μ M		% Inhibition at 1 μ M
			hA ₁ ^a	hA _{2A} ^a	hA ₃ ^a
43	<i>m</i> -F	7.4	73	58	23
44	<i>p</i> -F	7.3	92	56	33
45	<i>p</i> -CF ₃	12	66	21	14
46	<i>m</i> -OCF ₃	13	17	37	0

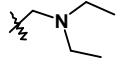
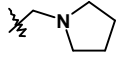
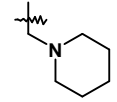
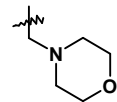
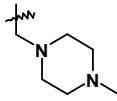
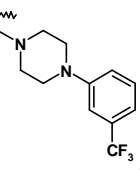
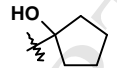
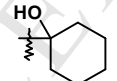
47	<i>p</i> -OCF ₃	9.9	84	49	32
48	<i>m</i> -CO ₂ H	190	NT	NT	NT
49	<i>p</i> -CO ₂ H	130	NT	NT	NT
50	<i>m</i> -F	3	53	60	0
51	<i>p</i> -F	1.6	77	55	0
52	<i>m</i> -CF ₃	2.2	26	39	0
53	<i>p</i> -CF ₃	1.3	89	39	15
54	<i>m</i> -OCF ₃	2.8	14	33	0
55	<i>p</i> -OCF ₃	1.6	88	46	17
56	<i>m</i> -CO ₂ H	48	NT	NT	NT

NT- not tested. ^aBinding affinities were determined by using membrane preparations from HEK-293 cells overexpressing the relevant human AdoR isoform. All data points were evaluated in triplicates. Each compound was evaluated at 8 concentrations with each data point in triplicates for K_i determination[45].

Table 4. Binding Affinity of Xanthine Derivatives with Different Substitution on Acetylene for A_{2B}, A₁, A_{2A} and A₃AdoRs



Compd	R	K_i (nM) hA _{2B} ^a	% Inhibition at 0.1 μ M		% Inhibition at 1 μ M
			hA ₁ ^a	hA _{2A} ^a	hA ₃ ^a

59	H	62	56	69	32
60	-CH ₃	23	42	60	NT
61		200	71	59	69
62		120	66	67	59
63		140	64	74	73
64		330	28	39	51
65		83	55	73	79
66		12	69	10	31
67		79	NT	NT	NT
68		100	NT	NT	NT

NT- not tested. ^aBinding affinities were determined by using membrane preparations from HEK-293 cells overexpressing the relevant human AdoR isoform. All data points were evaluated in triplicates. Each compound was evaluated at 8 concentrations with each data point in triplicates for K_i determination [45].

2.3. Drug Metabolism and Pharmacokinetic Studies

Based on affinity, potency and selectivity compound **29**, **36** and **46** were progressed for drug metabolism and pharmacokinetics (DMPK) evaluation and summarized in Table 5 [43]. All the three compounds were metabolically stable in mouse, rat and human liver microsomes and improved solubility. When dosed orally to mice at 10 mg/Kg, compound **46** showed better pharmacokinetics compared to compound **29**, with C_{\max} of 13 μM , systemic exposure $\text{AUC}_{(0-t)}$ of 60 $\mu\text{M}\cdot\text{h}$, $t_{1/2}$ of 6 h and oral bioavailability of 76%, Compound **36** displayed poor systemic exposure with high clearance in mice when dosed orally at 10 mg/Kg dose, and was found to be a substrate for Pgp ($B-A/A-B = 12$). Furthermore, compound **46** did not show any CYP liability ($\text{IC}_{50} > 10 \mu\text{M}$), cytotoxicity in MDCK and HepG2 cells ($\text{IC}_{50} > 100 \mu\text{M}$), or any significant hERG inhibition ($\text{IC}_{50} > 25 \mu\text{M}$).

Table 5. Oral Pharmacokinetic Profile of Compounds **29**, **36** and **46** in C57BL/6J Mice at 10mg/Kg^a

Compd	C_{\max} (μM)	$\text{AUC}_{(0-t)}$ ($\mu\text{M}\cdot\text{h}$)	$t_{1/2}$ (h)	%F	Solubility (μM) ^b
29	6.6	67	5	42	<6
36	1.9	2.2	1.8	10	529
46	13	60	6.1	76	21

^aPO formulation for **29** and **46**: DMAC(10%), CrEL(10%), PEG300(10%), MQ water (qs), pH ~9; for **36**: DMSO(10%), CrEL(10%), PEG300(10%), MQ water (qs), pH ~7; ^bAqueous solubility at pH 7.4

2.4. Molecular Docking analysis

As compound **46** showed good binding affinity, selectivity and acceptable pharmacokinetic properties, we were interested to understand the binding mode of this compound (**46**) in conjunction with reference compound **5**. Molecular docking analysis revealed that both the compounds had similar binding mode with good overlay and forming same intermolecular interactions with the A_{2B} AdoR binding pocket residues formed by transmembrane region TM3, TM5, TM6 and TM7 and extracellular loop ECL2 (Figure 2a). Moreover, both the compounds showed comparable docking score (Gold Chemscore DG was -26.03 and -26.88 for compounds **5** and **46**, respectively). It was identified that compound **46** is an

extended analog of **5**, where acetylene linker of the former is mimicking the northern phenyl ring of the later (Figure 2a). Both the compounds xanthine ring showed hydrogen bonding with a key residue Asn254 (TM6) and π - π interaction with Phe173 (ECL2). N-1 ethyl and N-3 propyl of the compounds accommodate well in the hydrophobic pocket. Northern phenyl ring of the compounds formed hydrophobic interaction with the ECL2 residue Leu172, whereas CF₃ group exposed in the bulk solvent. 2D interaction diagram of compound **46** is illustrated in Figure 2b. This analysis demonstrates the important molecular recognition interactions required for the A_{2B}AdoR activity.

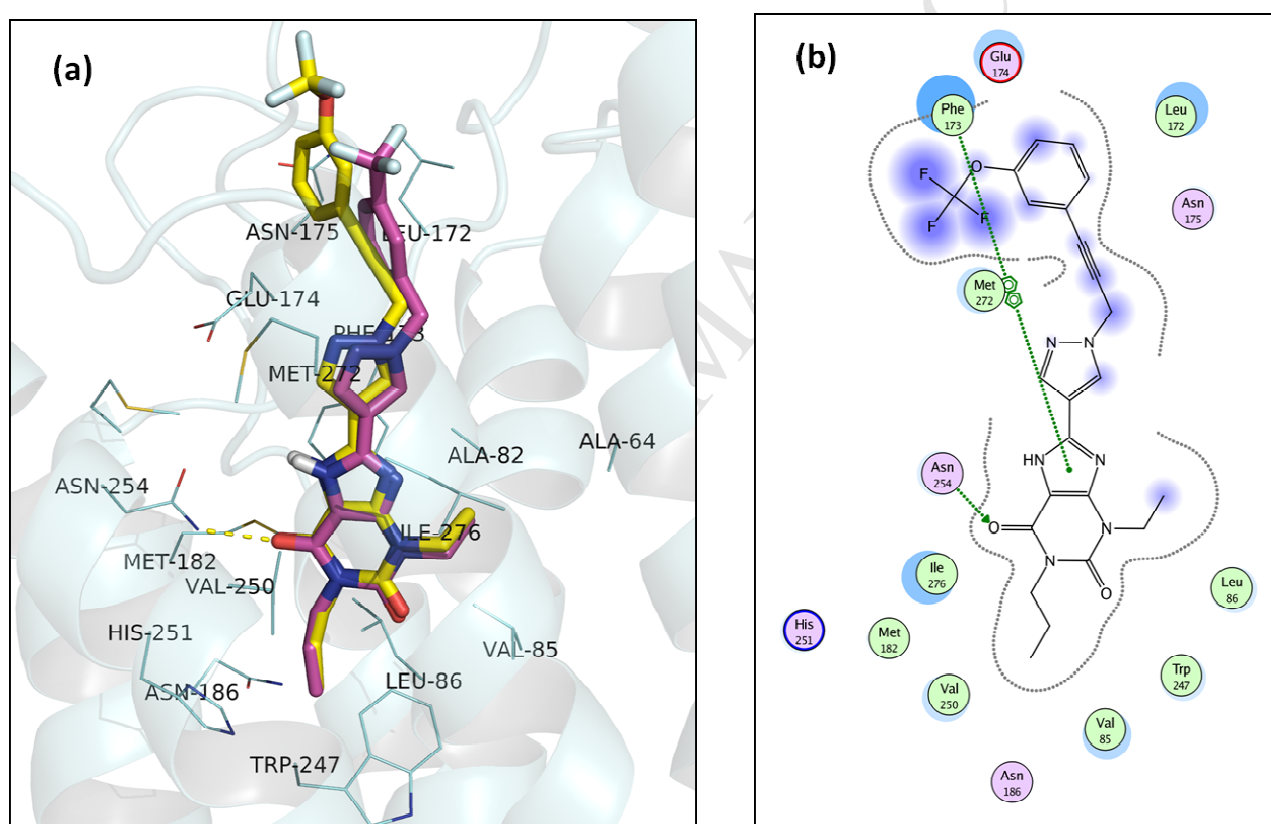
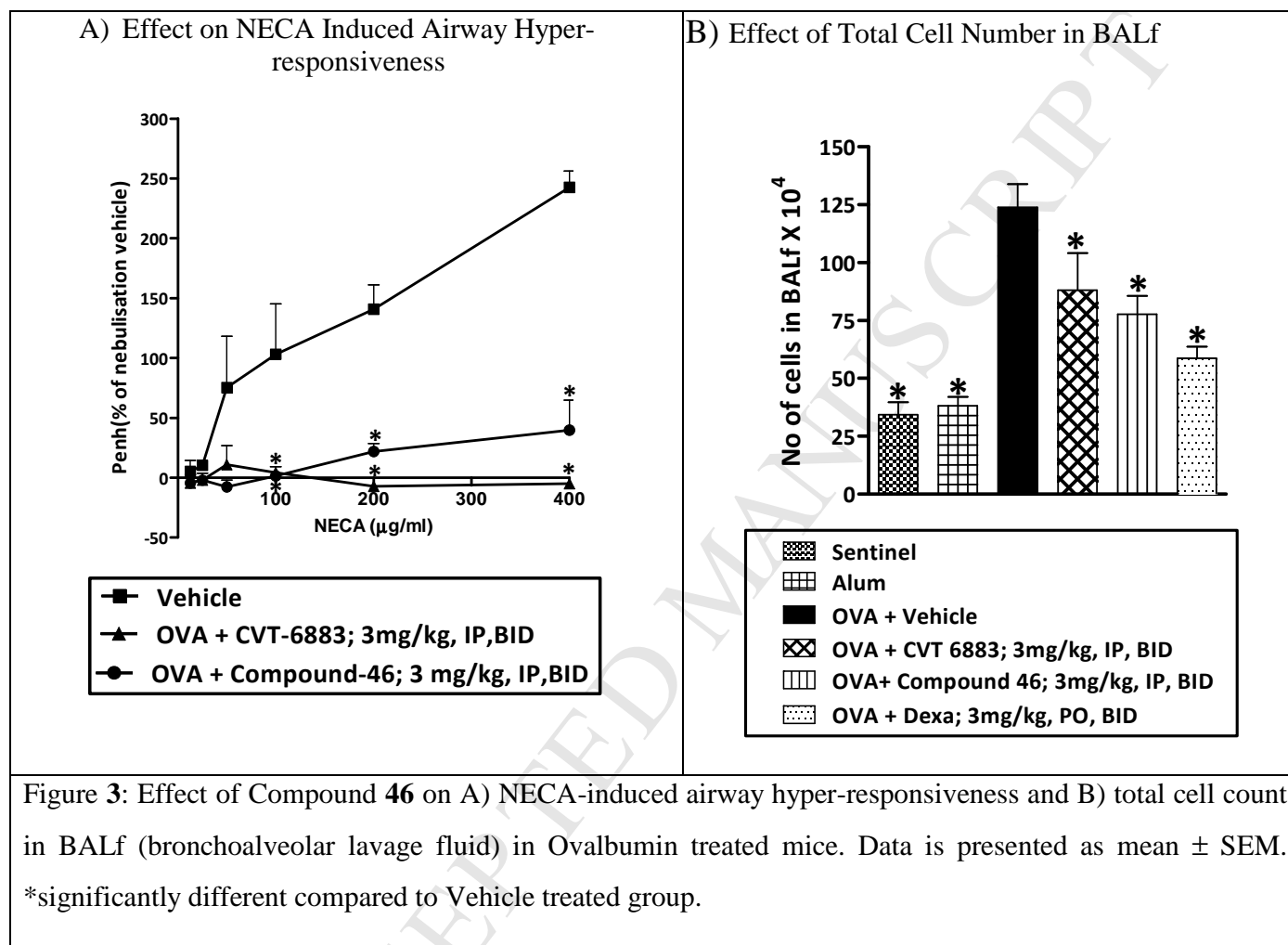


Figure 2. (a) Overlay of docking poses of the reference compound **5** (magenta) and the synthesized novel active compound **46** (yellow) in the homology modeled A_{2B}AdoR binding site (cyan cartoon representation). (b) 2D interaction diagram of compound **46** (hydrophobic residues are shown in green color and polar residues in pink).

2.5. *In vivo* efficacy study

Compound **46**, when evaluated for *in vivo* efficacy (Figure 3), showed reduction of increased inflammatory cells in ovalbumin-induced allergy model in mice, and significantly inhibited NECA-induced airway hyper-responsiveness [43].



3. Conclusion

A focused SAR study on 8-(1-prop-2-ynyl-1H-pyrazol-4-yl)-xanthine derivatives led to the identification of novel, potent and selective A_{2B} AdoR antagonists. Compound **46**, 3-ethyl-1-propyl-8-{1-[3-(3-trifluoromethoxy-phenyl)-prop-2-ynyl]-1H-pyrazol-4-yl}-xanthine emerged as the best compound in terms of affinity and selectivity over other subtypes for A_{2B} AdoR, solubility and PK. SAR study also led to identification of potent A_{2B} AdoR antagonist **36** with good aqueous solubility.

Compound **46** showed high binding affinity ($K_i = 13$ nM) and great selectivity over other AdoR subtypes. It was also potent with K_i of 8 nM in cAMP assay and IC_{50} 107 nM in the IL-6 assay, and showed good PK profile. Furthermore, compound **46** showed significant *in vivo* efficacy in the ovalbumin-induced allergic asthma model in mice. Further development around this series is in progress and will be reported in a due course of time.

4. Experimental section

4.1. General

Commercial chemicals and solvents were of reagent grade and were used without further purification. Anhydrous solvents were used without further drying. The following abbreviations are used for reagent and solvents: DCM-dichloromethane; DMF-dimethyl formamide; DMSO-dimethyl sulfoxide; EtOAc-ethyl acetate; EtOH-Ethanol; and MeOH-methanol. Globe chemie silica gel (100-200 or 230-400 mesh) was used for column chromatography. Analtech thin layer chromatography plates (20 x 20 cm, 2000 microns) were used for preparative thin layer chromatography. Proton NMR (1H NMR) spectra were recorded on a Varian 400 spectrometer (400 MHz). Solutions were typically prepared in either deuterated dimethyl sulfoxide (DMSO- d_6), deuterated methanol (CD $_3$ OD) or deuterated chloroform (CDCl $_3$). Chemical shifts are reported in δ units (parts per million) downfield from tetramethylsilane and are assigned as singlet (s), doublet (d), doublet of doublet (dd), triplet (t), quartet (q) and multiplets (m), and broad (br). Coupling constants (J) are reported in Hertz (Hz). Mass spectra (MS) were recorded on Agilent 6110. HPLC were recorded on Agilent RRLC using Eclipse XOB-C18 (250x4.6) mm Su column and 0.05 % fumaric acid (aq.) and acetonitrile as mobile phase with flow rate of 1ml/min at 30 °C for run time of 17 minutes and the HPLC purity is $\geq 95\%$ unless otherwise stated.

4.2. Synthesis

Preparation of 1,3-Dipropyl-8-{1-[3-(3-trifluoromethoxy-phenyl)-prop-2-ynyl]-1H-pyrazol-4-yl}-3,7-dihydro-purine-2,6-dione (29).

Preparation of 3-(3-Trifluoromethoxy-phenyl)-prop-2-yn-1-ol: A mixture of propargyl alcohol (1.0g, 18mmol), 1-Iodo-3-trifluoromethoxy-benzene (5.14g, 18mmol), copper iodide (0.342g, 1.8mmol), dichlorobis (triphenylphosphine) palladium (II) (0.632g, 0.9 mmol), diethylamine (30ml) was degassed for 10min. and stirred for 20h at 25-25 °C. Excess of diethyl amine was distilled off under vacuum. The residue was diluted with water (50ml) and extracted with ethyl acetate (3 X 50ml). The organic layer was washed with brine solution and dried over Na₂SO₄. The solvent was evaporated and the crude product was purified by column chromatography (10% Ethyl acetate in hexane) to obtain pure 3-(3-Trifluoromethoxy-phenyl)-prop-2-yn-1-ol (3.8g, 100 %). ¹HNMR (CDCl₃): δ 1.71 (t, *J*= 6Hz, 1H); 4.52 (d, *J*= 6Hz, 2H); 7.20 (d, *J*=7.2Hz, 1H); 7.28-7.39 (m, 3H).

Preparation of 1-(3-Bromo-prop-1-ynyl)-3-trifluoromethoxy-benzene: 3-(3-Trifluoromethoxy-phenyl)-prop-2-yn-1-ol (3.9g, 18mmol) was taken in DCM (50ml). The reaction mixture was then cooled to -5-0 °C. Tribromo phosphine (1ml, 11mmol) was added slowly at -5-0 °C and stirred at the same temperature for 3h. The reaction mixture was quenched with saturated NaHCO₃ solution and the organic layer was separated. The aqueous layer was extracted with DCM (2 X 40ml). The combined organic layer was washed with saturated brine solution, dried over Na₂SO₄, and evaporated under vacuum to get 1-(3-Bromo-prop-1-ynyl)-3-trifluoromethoxy-benzene (2.97g, 60%). ¹HNMR (CDCl₃): δ 4.12 (s, 2H); 7.20 (d, *J*= 6.8Hz, 1H); 7.30 (s, 1H); 7.34-7.39 (m, 2H); MS (*m/z*) (M⁺+1): 279.3.

Preparation of 1, 3-Dipropyl-8-{1-[3-(3-trifluoromethoxy-phenyl)-prop-2-ynyl]-1H-pyrazol-4-yl}-7-(2-trimethylsilyl-ethoxymethyl)-3, 7-dihydro-purine-2, 6-dione: A mixture of 1, 3-Dipropyl-8-(1H-pyrazol-4-yl)-7-(2-trimethylsilyl-ethoxymethyl)-3,7-dihydro-purine-2,6-dione **11d**³⁶ (1.0g, 2.3mmol), 1-(3-Bromo-prop-1-ynyl)-3-trifluoromethoxy-benzene (0.829g, 3.0mmol), K₂CO₃ (0.731mg, 5.3mmol) and acetone (50ml) were refluxed at 80 °C for 5h. The reaction mixture was cooled to room temperature and the solid K₂CO₃ was filtered off and evaporated the organic solvent under vacuum. The residue obtained was purified by column chromatography (2% methanol in dichloromethane) to get pure 1,3-

Dipropyl-8-{1-[3-(3-trifluoromethoxy-phenyl)-prop-2-ynyl]-1H-pyrazol-4-yl}-7-(2-trimethylsilyl-ethoxymethyl)-3,7-dihydro-purine-2,6-dione (1.5g, 100%). ¹HNMR (DMSO *d*₆): δ -0.01 (s, 9H); 0.94-1.03 (m, 8H); 1.68-1.73 (m, 2H); 1.80-1.87 (m, 2H); 3.83 (t, *J*= 8Hz, 2H); 4.01 (t, *J*= 7.6Hz, 2H); 4.13 (t, *J*= 7.2Hz, 2H); 5.26 (s, 2H); 5.81 (s, 2H); 7.35-7.42 (m, 4H); 8.19 (s, 1H); 8.40 (s, 1H); MS (*m/z*) (*M*⁺+1): 631.4

Preparation of 1,3-Dipropyl-8-{1-[3-(3-trifluoromethoxy-phenyl)-prop-2-ynyl]-1H-pyrazol-4-yl}-7-(2-trimethylsilyl-ethoxymethyl)-3,7-dihydro-purine-2,6-dione: 1,3-Dipropyl-8-{1-[3-(3-trifluoromethoxy-phenyl)-prop-2-ynyl]-1H-pyrazol-4-yl}-7-(2-trimethylsilyl-ethoxymethyl)-3,7-dihydro-purine-2,6-dione (1.4g, 2.2mmol) in EtOH (40mL) was treated with 2N HCl (20mL) and heated at 80 °C for 2h. The reaction mixture was concentrated in vacuo, and the residue was triturated with diethyl ether to afford 1,3-Dipropyl-8-{1-[3-(3-trifluoromethoxy-phenyl)-prop-2-ynyl]-1H-pyrazol-4-yl}-3,7-dihydro-purine-2,6-dione (0.915g, 80%) as a white solid. M.P. 199-200 °C; ¹HNMR (DMSO *d*₆): δ 0.85-0.91 (m, 6H); 1.54-1.60 (m, 2H); 1.69-1.75 (m, 2H); 3.85 (t, *J*= 7.2Hz, 2H); 3.98 (t, *J*= 7.2Hz, 2H); 5.42 (s, 2H); 7.45-7.50 (m, 2H); 7.54-7.56 (m, 2H); 8.12 (s, 1H); 8.53 (s, 1H); 13.59 (s, 1H); ¹³C NMR (DMSO-*d*₆, 100MHz): δ 153.8, 150.6, 148.4, 148.2, 145.0, 138.3, 131.0, 130.9, 129.7, 124.0, 123.4, 122.1, 118.7, 112.7, 106.3, 85.3, 83.2, 44.3, 42.1, 41.7, 20.8, 11.2, 11.0, MS (*m/z*) (*M*⁺+1): 501.2; HPLC purity 100%.

4.2.1. Radioligand Binding for Adenosine Receptors A₁, A_{2A}, A_{2B} and A₃.

Human adenosine receptor (A₁, A_{2A}, A_{2B} and A₃) cDNA was stably transfected into HEK-293 cells (referred to as HEK-A₁, HEK-A_{2A}, HEK-A_{2B}, HEK-A₃ cells). The HEK-293 cell was obtained from ATCC. The cells monolayer was washed with PBS once and harvested in a buffer containing 150 mM NaCl, 1 mM EDTA, 50 mM Tris, pH 7.4 (10 mM EDTA, 10 mM HEPES, pH 7.4 for HEK-A₃) at 1500 rpm for 5 min at room temperature. The cell pellet was incubated in sonication buffer containing 1 mM EDTA, 5 mM Tris, pH 7.4 (1 mM EDTA, 10 mM HEPES, pH-7.4 for HEK-A₃) for 10 mins at 4 oC followed by sonication on ice for 6 min. The lysate was centrifuged at 1000 x g for 10 min at 4 oC and the pellet was discarded. The supernatant was centrifuged at 49,000 x g for 45 min at 4 oC.

The resultant protein pellet was resuspended in sonication buffer supplemented with 1 U/ml adenosine deaminase (ADA, Roche) and incubated for 30 min at room temperature with constant mixing. The protein was washed twice with same buffer at 49,000 x g for 45 min at 4 °C and the final protein was stored in 50 mM Tris, pH 7.4 supplemented with 1 U/mL ADA and 10 % sucrose (1 mM EDTA, 5 mM Tris, pH 7.4, 1 U/ml ADA and 10% sucrose for HEK-A3). The protein concentration was estimated by Bradford assay and aliquots were stored at -80 °C.

The binding affinity and selectivity of test compounds was determined using radioligand binding assays. DPCPX (8-Cyclopentyl-1,3-dipropylxanthine, for A₁AdoR), Preladenant [2-(2-furanyl)-7-(2-(4-(4-(2-methoxyethoxy)phenyl)-1-piperazinyl)ethyl)-7H-pyrazolo(4,3-e)(1,2,4)triazolo(1,5-c)pyrimidine-5-amine, for A_{2A}AdoR], 3-Ethyl-3,9-dihydro-1-propyl-8-[1-[[3-(trifluoromethyl)phenyl]methyl]-1H-pyrazol-4-yl]-1H-purine-2,6-dione (CVT-6883, A_{2B}AdoR) and 3-Ethyl-5-benzyl-2-methyl-4-phenylethynyl-6-phenyl-1,4-(±)-dihydropyridine-3,5-dicarboxylate (MRS-119, A₃AdoR) were used as internal standards. Competition radioligand binding assays were started by mixing 1 nM [3H]-DPCPX (A1), 1 nM [2-3H]-4-(2-[7-amino-2-{2-furyl}{1,2,4}triazolo{2,3-a}{1,3,5,}triazin-5-yl amino]ethyl)phenol ([3H]ZM241385) (A2A), 35 1.6 nM radiolabelled N-(4-Cyanophenyl)-2-[4-(2,3,6,7-tetrahydro-2,6-dioxo-1,3-dipropyl-1H-purin-8-yl)phenoxy]acetamide ([3H]-MRS-1754) (A2B) or 2 nM [3H]-HEMADO (A3) with various concentrations of test compounds (and the respective membranes in assay buffer containing 50 mM Tris pH 7.4, 1 mM EDTA (A1), 50 mM Tris, pH 7.4, 10 mM MgCl₂, 1 mM EDTA, 1 U/ml ADA (A2A, A3) or 50 mM Tris pH 6.5, 5 mM MgCl₂, 1 mM EDTA (A2B) supplemented with 1 U/ml ADA. The assays were incubated at room temperature for 90 min with gentle agitation, stopped by filtration using a Harvester (Molecular Devices), and washed four times with ice-cold 50 mM Tris (pH 7.4). Nonspecific binding was determined in the presence of 100 μM NECA. The affinities of compounds (i.e., K_i values) were calculated using GraphPad software.

cAMP Assays: The functional activity of compounds was determined by evaluating the changes in cAMP levels post agonist treatment in HEK-293 cells over-expressing human A_{2B}AdoR. A 24 hour culture of cells was treated with 1 U/mL of ADA in DMEM supplemented with 10% FBS for 90 minutes at 37°C and 5% CO₂. Cells were harvested using cell dissociation buffer (Sigma), washed with incomplete DMEM and incubated with increasing concentrations of test compound for 15 minutes in DMEM supplemented with 1U/ml ADA at room temperature. The cAMP levels were induced using A_{2B}AdoR agonist NECA for 15 minutes. The levels of cAMP were detected and estimated as per manufacturer's instruction using the Cisbio HTRF cAMP kit. The FRET between d2-labeled cAMP and cryptate labeled anti-cAMP antibody was read in HTRF mode in a Flex Station III (Molecular Devices) using an excitation maximum of 313 nm and emission maxima of 620 nm and 665 nm. Data was analyzed using GraphPad Prism software to determine IC₅₀ and K_i values.

4.2.2. *Molecular Modeling*

Homology model development

In the absence of any experimentally (X-ray or NMR) determined three dimensional (3d) structure of human A_{2B}AdoR, homology model of this receptor was built using MOE program [46] by implementing the standard protocol. On the basis of lowest E value, good Z score and highest percentage identity (61%) with the query protein, PDB ID: 4E1Y (X-ray crystal structure of A_{2A}AdoR with small molecule antagonist ZM241385) [47] was found to be the most suitable template for building the homology model of human A_{2B}AdoR. Among the several other crystal structures of A_{2A}AdoR in the Protein Data Bank (PDB), this structure was particularly selected due to its high resolution and better overall B-factor. Initially, 100 models were generated and the best model was selected on the basis of Generalized Born/Volume Integral (GB/VI) score, C α RMSD with the template protein, contact energy and packing score. The best model was checked for its stereochemistry using Ramachandran plot. Model refinement and minimization was done using Amber99 (R-Field) force field. The template ligand ZM241385 coordinates were transferred in the homology modeled structure of A_{2B}AdoR in order to define the binding site.

Molecular Docking

Ligands were built in MOE, hydrogens were added, partial charges were assigned and minimized using MMF94X force field. Molecular docking was performed by GOLD 5.2.2. (Genetic Optimization for Ligand Docking) program from Cambridge Crystallographic Data Centre (CCDC), UK [47] using standard protocol as mentioned elsewhere. The binding site of modeled A2BAdoR for the purpose of docking was defined by selecting the bound ligand (ZM241385). All the atoms within 6 Å range from the centre of bound ligand were selected in order to cover all the residues of active site. Subsequently, all the H-bond donors/acceptors were forced to be treated as solvent accessible. A maximum of 10 docking GA runs per molecule were performed, allowing all the poses to generate and sorted by using ChemScore fitness scoring function. All other parameters were kept at their default values for the docking. Most plausible docking poses for the compounds were selected by visual inspection on the basis of binding orientation, key interactions and Gold Chemscore DG.

Appendix A. Supplementary data

The contents of supporting information include the following: (1) experimental procedures and characterization (3) ¹H NMR/¹³C NMR spectra of selected compounds

Acknowledgements

Authors are grateful to the senior management of the Advinus Group for its support and encouragement. Analytical departments are acknowledged for their help during this work. We thank Dr. Anup Ranade for managing intellectual property - Advinus publication no. ADV-A-040

References

[1] Ralevic, V.; Burnstock G. Receptors for Purines and Pyrimidines. *Pharmacol. Rev.* **1998**, *50*, 413-492.

- [2] Muller, C. E.; Stein, B. Adenosine Receptor Antagonists: Structures and Potential Therapeutic Applications. *Curr. Pharm. Des.* **1996**, *2*, 501-530.
- [3] Linden, J. Molecular Approach to Adenosine Receptors: Receptor Mediated Mechanisms of Tissue Protection. *Annu. Rev. Pharmacol. Toxicol.* **2001**, *41*, 775-787.
- [4] Fozard, J. R.; Hannon, J. P. Adenosine Receptor Ligands: Potential as Therapeutic Agents in Asthma and COPD. *Pulm. Pharmacol. Ther.* **1999**, *12*, 111-114.
- [5] Feoktistov, I.; Biaggioni, I. Adenosine A_{2B} Receptors. *Pharmacol. Rev.* **1997**, *49*, 381-402.
- [6] Baraldi, P.G.; Romagnoli, R.; Preti, D.; Fruttarolo, F.; Carrion, M.D.; Tabizi, M.A. Ligands for A_{2B} Adenosine Receptor Subtype. *Curr. Med. Chem.*, **2006**, *13*, 3467-3482.
- [7] Feoktistov, I.; Murray, J.J.; Biaggioni, I. Positive Modulation of Intracellular Ca²⁺ Levels by Adenosine A_{2B} Receptors, Prostacyclin, and Prostaglandin E1 via a Cholera Toxin-Sensitive Mechanism in Human Erythroleukemia Cells. *Mol. Pharmacol.*, **1994**, *45*, 1160-1167.
- [8] Mogul, D.J.; Adams, M.E.; Fox, A.P. Differential Activation of Adenosine Receptors Decreases N-Type but Potentiates P-Type Ca²⁺ Current in Hippocampal CA3 Neurons. *Neuron*, **1993**, *10*, 327-334.
- [9] Auchampach, J.A.; Caughey, G.H.; Linden, J. A_{2B} and not A₃ Adenosine Receptors Mediate Degranulation of Canine BR Mastocytoma Cells. *Drug Dev. Res.*, **1996**, *38*, 147.
- [10] Auchampach, J. A.; Jin, X.; Wan, T. C.; Caughey, G. H.; Linden J. Canine Mast Cell Adenosine Receptors: Cloning and Expression of the A₃ Receptor and Evidence that Degranulation is Mediated by the A_{2B} Receptor. *Mol. Pharmacol.* **1997**, *52*, 846-860.
- [11] Gurden, M. F.; Cates, J.; Ellis, F.; Evans, B.; Foster, M.; Hornby, E.; Kennedy, I.; Martin, D.P.; Strong, P.; Vardey, C. Y.; Wheeldon, A. Functional Characterization of Three Adenosine Receptor Types. *Br. J. Pharmacol.* **1993**, *109*, 693-698.

- [12] Clancey, J. P.; Ruiz, F. E.; Sorscher, E. J. Adenosine and its Nucleotides Activate Wild-Type and R117H CFTR Through an A_{2B} Receptor-Coupled Pathway. *Am. J. Physiol.* **1999**, *276*, C361-C369.
- [13] Strohmeier, G. R.; Reppert, S. M.; Lencer, W. I.; Madaa, J. L. The A_{2B} Adenosine Receptor Mediates Camp Responses to Adenosine Receptor Agonists in Human Intestinal Epithelia. *J. Biol. Chem.* **1995**, *270*, 2387-2394.
- [14] Dubey, R. K.; Gillespie, D. G.; Mi, Z.; Jackson, E. K. Adenosine Inhibits Growth of Human Aortic Smooth Muscle Cells via A_{2B} Receptors. *Hypertension* **1998**, *31*, 516-521.
- [15] Harada, H.; Asano, O.; Hoshino, Y.; Yoshikawa, S.; Matsukura, M.; Kabasawa, Y, Nijima, J.; Kotake, Y.; Watanabe, N.; Kawata, T.; Inoue, T.; Horizoe, T.; Yasuda, N.; Minami, H.; Nagata, K.; Murakami, M.; Nagaoka, J.; Kobayashi, S.; Tanaka, I.; Abe, S. 2-Alkynyl-8-Aryl-9-Methyladenines as Novel Adenosine Receptor Antagonists: Their Synthesis and Structure-Activity Relationships Toward Hepatic Glucose Production Induced via Agonism of the A_{2B} Receptor. *J. Med. Chem.* **2001**, *44*, 170-179.
- [16] Adair, T.H.; Cotton, R.; McMullan, M.R.; Li, W.; Gu, J.W. Adenosine Increases Plasma Levels of VEGF in Humans (Abstract). *FASEB J.*, **2001**, *15*, A277.
- [17] Marx, D.; Ezeamuzie, C. I.; Nieber, K.; Szenlenyi, I. Therapy of Bronchial Asthma with Adenosine Receptor Agonists or Antagonists. *Drug News Perspect.* **2001**, *14*, 89-100.
- [18] Feoktistov, I.; Palosa, R.; Holgate, S. T.; Biaggioni, I. Adenosine A_{2B} Receptors: A Novel Therapeutic Target in Asthma. *Trends Pharmacol. Sci.* **1998**, *19*, 148-153.
- [19] Ham, J.; Rees, D. A.; The Adenosine A_{2B} Receptor: Its Role in Inflammation, Endocrine, Metabolic & Immune Disorders – Drug Targets, **2008**, *8*, 244-254.
- [20] Jacobson, K.A.; Hoffman, C.; Cattabeni, F.; Abbracchio, M. P. Adenosine-Induced Cell Death: Evidence for Receptor-Mediated Signaling. *Apoptosis*, **1999**, *4*, 197-211.

- [21] Cushley, M.J.; Tattersfield, A.E.; Holgate, S.T. Inhaled Adenosine and Guanosine on Airway Resistance in Normal and Asthmatic Subjects. *Brit. J. Clin. Pharmacol.*, **1983**, *15*, 161-165.
- [22] Cushley, M.J.; Tattersfield, A.E.; Holgate, S.T. Adenosine-induced Bronchoconstriction in Asthma. Antagonism by Inhaled Theophylline. *Am. Rev. Respir. Dis.*, **1984**, *129*, 380-384.
- [23] Driver, A.G.; Kukoly, C.A.; Ali, C.S.; Mustafa, S.J. Adenosine in Bronchoalveolar Lavage Fluid in Asthma. *Am. Rev. Respir. Dis.*, **1993**, *148*, 91-97.
- [24] Huszar, E.; Vass, G; Vizi, E.; Csoma, Z.; Barat, E.; Molnar Vilagos, G.; Herjavec, I.; Horvath, I. Adenosine in Exhaled Breath Condensate in Healthy Volunteers and in Patients with Asthma. *Eur. Respir. J.*, **2002**, *20*, 1393-1398.
- [25] Chunn, J. L.; Molina, J. G.; Mi, T.; Xia, Y.; Kellems, R. E.; Blackburn, M. R. Adenosine-Dependent Pulmonary Fibrosis in Adenosine Deaminase-Deficient Mice. *J. Immunol.*, **2005**, *175*, 1937-1946.
- [26] Ma, B.; Blackburn, M.R.; Lee, C.G.; Homer, R.J.; Lui, W.; Flavell, R.A.; Boyden, L.; Lifton, R.P.; Sun, C.X.; Young, H.W.; Elias, J.A. Adenosine Metabolism and Murine Strain-Specific IL-4-Induced Inflammation, Emphysema, and Fibrosis. *J. Clin. Invest.*, **2006**, *116*, 1274-1283.
- [27] Ryzhov, S.; Goldstein, A.E.; Matafonov, A.; Zeng, D.; Biaggioni, I.; Feoktistov, I. Adenosine-Activated Mast Cells Induce IgE Synthesis by B Lymphocytes: An A_{2B}-Mediated Process Involving Th2 Cytokines IL-4 and IL-13 with Implications for Asthma. *J. Immunol.*, **2004**, *172*, 7726-7733.
- [28] Zhong, H.; Wu, Y.; Belardinelli, L.; Zeng, D. A_{2B} Adenosine Receptors Induce IL-19 from Bronchial Epithelial Cells Resulting in TNF-alpha Increase. *Am. J. Respir. Cell Mol. Biol.*, **2006**, *35*, 587-592.

- [29] Zhong, H.; Belardinelli, L.; Maa, T.; Feoktistov, I.; Biaggioni, I.; Zeng, D. A_{2B} Adenosine Receptors Increase Cytokine Release by Bronchial Smooth Muscle Cells. *Am. J. Respir. Cell Mol. Biol.*, **2004**, *30*, 118-125.
- [30] Zhong, H.; Belardinelli, L.; Maa, T.; Zeng, D. Synergy between A_{2B} Adenosine Receptors and Hypoxia in Activating Human Lung Fibroblasts. *Am. J. Respir. Cell Mol. Biol.*, **2005**, *32*, 2-8.
- [31] D'Alonzo, G. E. Theophylline Revisited. *Allergy Asthma. Proc.* **1996**, *17*, 335-339.
- [32] Jacobson, K. A.; Ijzerman, A. P.; Linden, J. 1,3-Dialkylxanthine Derivatives Having High Potency as Antagonists at Human A_{2B} Adenosine Receptors. *Drug Dev. Res.* **1999**, *47*, 45-53.
- [33] Beukers, M. W.; Meurs, I.; Ijzerman, A. P. Structure-Affinity Relationships of Adenosine A_{2B} Receptor Ligands. *Med. Res. Rev.* **2006**, *26*, 667-698.
- [34] Cacciari, B.; Pastorin, G.; Bolcato, C.; Spalluto, G.; Bacilieri, M.; Moro, S. A_{2B} Adenosine Receptor Antagonists: Recent Developments. *Mini-Rev. Med. Chem.* **2005**, *5*, 1053-1060.
- [35] Baraldi, P. G.; Tabrizi, M. A.; Preti, D.; Bovero, A.; Romagnoli, R.; Fruttarolo, F.; Zaid, N. A.; Moorman, A. R.; Varani, K.; Gessi, S.; Merighi, S.; Borea, P. A. Design, Synthesis, and Biological Evaluation of New 8-Heterocyclic Xanthine Derivatives as Highly Potent and Selective Human A_{2B} Adenosine Receptor Antagonists. *J. Med. Chem.* **2004**, *47*, 1434-1447.
- [36] Kalla, R.; Elzein, E.; Perry, T.; Li, X.; Palle, V.; Varkhedkar, V.; Gimbel, A.; Maa, T.; Zeng, D.; Zablocki, J. Novel 1,3-Disubstituted-8-(1-Benzyl-1H-Pyrazol-4-yl) Xanthines: High Affinity and Selective A_{2B} Adenosine Receptor Antagonists. *J. Med. Chem.* **2006**, *49*, 3682-3692.
- [37] Stefanachi, A.; Brea, J. M.; Cadavid, M. I.; Centeno, N. B.; Esteve, C.; Loza, M. I.; Martinez, A.; Nieto, R.; Raviña, E.; Sanz, F.; Segarra, V.; Sotelo, E.; Vidal, B.; Carotti, A. 1-, 3- and 8-Substituted-9-Deazaxanthines as Potent and Selective Antagonists at the Human A_{2B} Adenosine Receptor. *Biorg. Med. Chem.* **2008**, *16*, 2852-2869.

[38] Kim, Y.-C.; Ji, X.-d.; Melman, N.; Linden, J.; Jacobson, K. A. Anilide Derivatives of an 8-Phenylxanthine Carboxylic Congener are Highly Potent and Selective Antagonists at Human A_{2B} Adenosine Receptors. *J. Med. Chem.* **2000**, *43*, 1165-1172.

[39] Ji, X.; Kim, Y. C.; Ahern, D. G.; Linden, J.; Jacobson, K. A. [³H]-MRS 1754, A Selective Antagonist Radioligand for A_{2B} Adenosine Receptors. *Biochem. Pharmacol.* **2001**, *61*, 657-663.

[40] Elzein, E.; Kalla, R. V.; Li, X.; Perry, T.; Gimbel, A.; Zeng, D.; Lustig, D.; Leung, K.; Zablocki, J. Discovery of a Novel A_{2B} Adenosine Receptor Antagonist as a Clinical Candidate for Chronic Inflammatory Airway Diseases. *J. Med. Chem.* **2008**, *51*, 2267-2278.

[41] Mustafa, S. J.; Nadeem, A.; Fan, M.; Zhong, H.; Belardinelli, L.; Zeng, D. Effect of a Specific and Selective A_{2B} Adenosine Receptor Antagonist on Adenosine Agonist AMP and Allergen-Induced Airway Responsiveness and Cellular Influx in a Mouse Model of Asthma. *J. Pharmacol. Exp. Ther.* **2007**, *320*, 1246-1251.

[42] Sun, C.; Zhong, H.; Mohsenin, A.; Morschl, E.; Chunn, J. L.; Molina, J. G.; Belardinelli, L.; Zeng, D.; Blackburn, M. R. Role of A_{2B} Adenosine Receptor Signaling in Adenosine-Dependent Pulmonary Inflammation and Injury. *J. Clin. Invest.* **2006**, *116*, 2173-2182.

[43] Basu, S.; Barawkar, A. D.; Ramdas, V.; Waman, Y.; Patel, M.; Panmand, A.; Kumar, S.; Thorat, S.; Bonagiri, R.; Jadhav, D.; Mukhopadhyay, P.; Prasad, V.; Reddy, B. S.; Goswami, A.; Chaturvedi, S.; Menon, S.; Quraishi, A.; Ghosh, I.; Dusange, S.; Paliwal, S.; Kulkarni, A.; Karande, V.; Thakre, R.; Bedse, G.; Rouduri, S.; Gundu, J.; Palle, V. P.; Chugh, A.; Mookhtiar, K. A. A_{2B} adenosine receptor antagonists: Design, synthesis and biological evaluation of novel xanthine derivatives. *Eur. J. Med. Chem.* **2017**, *127*, 986-996.

[44] Kalla, R.; Elzein, E.; Perry, T.; Li, X.; Gimbel, A.; Yang, M.; Zeng, D.; Zablocki, J. Selective, High Affinity A_{2B} Adenosine Receptor Antagonists: N-1 Monosubstituted 8-(Pyrazol-4-yl)Xanthines. *Bioorg. Med. Chem. Lett.* **2008**, *18*, 1397-1401.

[45] Binding affinity for hA_{2B}AdoR was determined using [³H]-MRS-1754 as ligand; Binding affinity for hA₁AdoR was determined using [³H]-DPCPX as ligand; Binding affinity for hA_{2A}AdoR was determined using [³H]-ZM-241385 as ligand; and Binding affinity for hA₃AdoR was determined using [³H]-HEMADO as ligand.

[46] Molecular Operating Environment (MOE), 2013.08; Chemical Computing Group Inc., 1010 Sherbooke St. West, Suite #910, Montreal, QC, Canada, H3A 2R7, 2017.

[47] Liu, W.; Chun, E.; Thompson, A. A.; Chubukov, P.; Xu, F.; Katritch, V.; Han, G. W.; Roth, C. B.; Heitman, L. H.; IJzerman, A. P.; Cherezov, V.; Stevens, R. C. Structural Basis for Allosteric Regulation of GPCRs By Sodium Ions. *Science* **2012**, *337*, 232–236.

[48] Jones, G.; Willett, P.; Glen, R. C.; Leach A. R.; Taylor R. Development and Validation of a Genetic Algorithm for Flexible Docking. *J. Mol. Biol.* **1997**, *267*, 727-748.

Highlights

- To identify novel, potent and selective A_{2B}AdoR antagonists with in vivo efficacy
- Identified A_{2B}AdoR antagonists with very good functional potency and with improved pharmacokinetic properties
- Identified compound **36** with very good solubility
- Identified compound **46** with good pharmacokinetics properties and found to be efficacious in ovalbumin-induced allergic asthma model in mice